Video Article

Integrate Imaging Flow Cytometry and Transcriptomic Profiling to Evaluate Altered Endocytic CD1d Trafficking

Manju Sharma[1], Xiang Zhang[1], Shouxiong Huang[1]

[1]Department of Environmental Health, University of Cincinnati College of Medicine

Correspondence to: Xiang Zhang at xiang.zhang@uc.edu, Shouxiong Huang at shouxiong.huang@uc.edu

URL: https://www.jove.com/video/57528
DOI: doi:10.3791/57528

Keywords: Immunology and Infection, Issue 140, Imaging Flow Cytometry, ImageJ-Fiji, IDEAS, Transcriptomics, Pathway analysis, Cytoscape

Date Published: 10/29/2018

Citation: Sharma, M., Zhang, X., Huang, S. Integrate Imaging Flow Cytometry and Transcriptomic Profiling to Evaluate Altered Endocytic CD1d Trafficking. *J. Vis. Exp.* (140), e57528, doi:10.3791/57528 (2018).

Abstract

Populational analyses of the morphological and functional alteration of endocytic proteins are challenging due to the demand of image capture at a single cell level and statistical image analysis at a populational level. To overcome this difficulty, we used imaging flow cytometry and transcriptomic profiling (RNA-seq) to determine altered subcellular localization of the cluster of differentiation 1d protein (CD1d) associated with impaired endocytic gene expression in human dendritic cells (DCs), which were exposed to the common lipophilic air pollutant benzo[a]pyrene. The colocalization of CD1d and endocytic marker Lamp1 proteins from thousands of cell images captured with imaging flow cytometry was analyzed using IDEAS and ImageJ-Fiji programs. Numerous cellular images with co-stained CD1d and Lamp1 proteins were visualized after gating on $CD1d^{+}Lamp1^{+}$ DCs using IDEAS. The enhanced CD1d and Lamp1 colocalization upon BaP exposure was further demonstrated using thresholded scatterplots, tested with Mander's coefficients for co-localized intensity, and plotted based on the percentage of co-localized areas using ImageJ-Fiji. Our data provide an advantageous instrumental and bioinformatic approach to measure protein colocalization at both single and populational cellular levels, supporting an impaired functional outcome of transcriptomic alteration in pollutant-exposed human DCs.

Video Link

The video component of this article can be found at https://www.jove.com/video/57528/

Introduction

Antigen presentation typically involves intracellular protein trafficking, which has been often investigated using morphological characterization and phenotypic profiling of antigen presenting cells[1,2,3]. To integrate the advantages of imaging and phenotyping methods, we describe an imaging analysis platform at both single cell and population levels to demonstrate an altered protein colocalization in human dendritic cells (DCs). In peptide antigen presentation, major histocompatibility complex (MHC) class I molecules bind a short peptide (8-10 residues) in the endoplasmic reticulum to activate conventional $CD8^{+}$ T cells, while MHC class II molecules bind a relatively longer peptide (~20 residues) in endocytic compartments to activate conventional $CD4^{+}$ T cells[1,4]. In contrast, lipid-specific T cells are activated by CD1 proteins with lipid antigens loaded mainly in endocytic compartments[5,6]. Lipid antigen presentation requires the supply of lipid metabolites produced in lipid metabolism[7,8,9,10] and the loading of functional lipid metabolites to CD1 proteins in endocytic compartments[5,6]. In this context, various cellular factors modulating lipid antigen presentation, especially in environmental exposure of lipophilic pollutants and immune disorders, are critical to be defined. In this study, we used transcriptomic analysis, image profiling, and cellular and populational imaging analysis of human monocyte-derived DCs to determine the endocytic protein trafficking contributing to lipid antigen presentation in pollutant exposure. Certainly, this combined platform can be applied to studying subcellular protein trafficking and colocalization in different biological processes.

Technically, subcellular protein localization was usually demonstrated using confocal microscopy and statistically analyzed in a limited number of detected cells[1,2,3,11]. Moreover, flow cytometry has been broadly applied to gate cell populations with co-stained signals of multiple proteins at a cellular level[12]; however, this lacks a detailed visualization of subcellular protein colocalization. To achieve comprehensive and statistical analyses of percentage protein colocalization at both cellular and population levels, we incorporate imaging profiling and analysis approaches to determine the features of protein colocalization with biological relevance. Specifically, we use imaging flow cytometry to detect the colocalization of CD1d and lysosomal-associated membrane protein 1 (Lamp1) proteins in this study. Quantitative analysis of colocalized molecules was previously difficult to be performed at a populational scale. In this study, we adapted the ImageJ-Fiji program to examine the percentage of protein colocalization with a large number of co-stained cells at both populational and individual cellular levels. Specifically, we measured co-localized areas, intensity, and populational size to support the conclusion that the CD1d protein was largely retained in late endocytic compartments of human DCs in exposure to a lipophilic pollutant benzo[a]pyrene (BaP)[13]. This combined cellular and population imaging analysis provided highly reproducible, comprehensive, and statistically significant results of CD1d-Lamp1 colocalization relevant to inhibited lipid antigen presentation.

The transcriptome of BaP-exposed human DCs strongly supported the hypothesis that endocytic lipid metabolism and CD1d endocytic trafficking were impaired in BaP exposure. To test this hypothesis, we applied imaging flow cytometry to profile the images of DC population that were

co-stained with multiple proteins including CD1d, endocytic markers, and DC markers. Finally, co-stained cells were statistically analyzed to demonstrate the percentage of intensity and areas of CD1d and Lamp1 colocalization.

Protocol

Human protocols in this study were approved by the Institutional Review Board of the University of Cincinnati and all methods were performed in accordance with the relevant guidelines and regulations. Blood samples from healthy donors were obtained from the Hoxworth Blood Center at the University of Cincinnati Medical Center.

1. Transcriptomic Profiling of Pollutant-exposed Human Monocyte-derived DCs

1. Total RNA extraction of BaP-exposed DCs
    1. Differentiate human DCs using cytokines GM-CSF and IL-4, and expose DCs to BaP for 4 days[13].
    2. Sort BaP-exposed DCs using flow cytometry based on the surface expressed markers (Lineage$^-$HLA-DR$^+$), the majority of which consists of conventional DCs (CD11c$^+$CD1c$^+$)[13]. Typically, sort 10,000 DCs into culture medium containing 10% FBS, centrifuge DCs at 600 x g and 4 °C for 6 min, and immediately remove the supernatant by aspiration using a 1 mL pipette tip.
    3. Once the supernatant is removed by aspiration, lyse the cell pellet by adding 0.4 mL of Lysis/Binding Buffer from the RNA isolation kit for storage in -80 °C before RNA extraction.
    4. Use the RNA isolation kit with the total RNA extraction protocol to extract the total RNA[14]. Measure the RNA integrity using a Bioanalyzer[15].

2. Transcriptomic analysis of sorted DCs (**Figure 1A**)
    1. Prepare the library for RNA-seq using a RNA Library preparation kit. In short, fragment the isolated poly-A RNA (~200 bp), reverse transcribe the fragments to the 1st strand of the cDNA, and follow by the second strand cDNA synthesis labeled with dUTP.
    2. Ligate double strand cDNA to the adapter with a stem-loop structure after bead purification, end-repairing and dA-tailing. Excise the uracil residues in the 2nd strand of the cDNA and adapter loop with USER (Uracil-Specific Excision Reagent) enzyme to maintain strand specificity and open the adapter loop for PCR.
        1. Perform 13 cycles of PCR using universal and index-specific primers to enrich the indexed library. Clean up the library and run on a Bioanalyzer DNA High Sensitivity chip to check the library quality and size distribution.
    3. Use a library quantification kit and a real-time PCR system combined with library size information to calculate library concentration *via* a standard curve method.
    4. Proportionally pool individually indexed compatible libraries and adjust the final total concentration to 15 pM. Perform library cluster generation and sequence the library at a setting of single read 1x 50 bp to generate ~25 million reads per sample.

3. Sequencing
    1. Load the sequencing and indexing reagents to the SBS and PE reagent racks, respectively. Place the reagents in a laboratory-grade water bath for 1 h until all the ice has melted and the reagents in each bottle/tube are mixed properly.
    2. Prepare the ICB mix by adding the thawed dye and -20 °C enzyme to the bottle and mix. Prepare a NaOH solution according to the sequencing instructions. Place all reagents at 4 °C until ready to use.
    3. During the 1 h waiting period, power on the sequencer. Wait for the DONOTEJECT drive to appear and connect the computer to a network drive.
    4. Launch the sequencer control software.
    5. Prepare 2 L of Maintenance Wash solution that contains 0.5% Tween 20 and 0.03% ProClin 300 in laboratory-grade water.
    6. In the SBS reagent rack, add ~100 mL of Maintenance Wash solution to each of the 8 bottles, and screw funnel caps to the bottles. In the PE reagent rack, add ~12 mL of Maintenance Wash solution to each of the ten 15 mL conical tubes, and discard the caps.
    7. Load the two racks with the solution filled bottles/tubes to the sequencer.
    8. From the sequencer control software, choose the Maintenance Wash; follow the instructions on screen to clean the sequencer fluid system until the process is completed.
    9. Start a New Run in the *"SEQUENCE"* tab from the software; direct the output data to a network drive. Choose parameters for single read 1x 50 bp with single index multiplexed libraries.
    10. Optionally, log into the BaseSpace Sequence Hub so that the sequencing status can be remotely monitored via a computer or smart phone.
    11. Upload a Sample Sheet for demultiplexing and provide reagent information according to the software requirement.
    12. Load SBS and PE reagents to the sequencer. Prime the system with a used flow cell (~15 min).
    13. Once the cluster generation is completed (~4.5 h), take the flow cell out, lightly spray the flow cell with water, and wipe it dry using lens paper. Lightly spray the flow cell with 95% ethanol and wipe it dry. Check against a light to make sure that the surface is clean without debris or salt residue.
    14. After the Prime step is completed, load the clustered flow cell and start the sequencing. The Sequence Analysis Viewer software will automatically be started.
    15. Monitor the sequencing data quality via SAV including cluster density, reads pass filter, cluster pass filter %, % ≥Q30, Legacy phase/prophase %, indexing QC, *etc.* This helps to understand the data quality and troubleshoot.
    16. Change the flow cell gasket and perform a Maintenance Wash after the sequencing is completed. The sequencer is ready for the next run.

4. Bioinformatic analysis
    1. Perform bioinformatics RNA-seq data analysis[13].

2. Pathway Analysis of Transcriptomic Profiles (Figure 1B)

1. Use an edgeR Bioconductor to compare resultant gene expression intensity counts between BaP-exposed and non-exposed DCs from three donors. Then, identify differentially expressed genes between BaP-exposed and non-exposed DCs based on the absolute fold change (>2 folds) and the false discovery rate (FDR)-adjusted *p*-values (<0.05).
2. To predict the functional clusters of differentially expressed genes, use the ToppCluster software package to search the altered genes against several databases including KEGG and REACTOME and generate clustering data. ToppCluster uses the hypergeometric test to obtain functional enrichment via the gene list enrichment analysis[16].
3. Further input the results from these function clusters to Cytoscape[17,18] Version 3.3.0, a broadly used open source software platform for visualizing complex networks. Thus, the genes involved in different clusters or pathways, including endocytic clusters and lipid metabolism, are shown in a network with color annotation of the averaged fold change of gene expression (**Figure 1B**)[13].

3. Imaging Flow Cytometry of CD1d and Lamp1 Colocalization

1. Antibody labeling of BaP-exposed DCs
    1. Expose 0.5 x 10^6 human DCs to 5.94 mM BaP for 4 days at 37 °C in 2 mL of complete Dulbecco's Modified Eagle's Medium. Harvest DCs by centrifugation at 400 x g for 10 min. Block the differentiated DCs by incubating cells with human serum blocker and anti-human Fc receptor antibodies for 10 min in ice, including anti-human CD16, CD32, and CD64 antibodies.
    2. Incubate Brilliant Violet 421-anti-CD1c (L161), phycoerythrin/cyanine dye 7 (PE/Cy7)-anti-HLA-DR, and PE/Cy5-anti-CD11c with DCs for 20 min in ice. **Table 1** shows this list of antibodies.
    3. Fix DCs with 4% paraformaldehyde in PBS and permeabilize them with Permeabilization Wash Buffer. Perform the intracellular staining with a mixture of PE-labeled purified anti-human CD1d (51.1) and Alexa Fluor 647-labeled anti-Lamp1 (CD107a) (H4A3).

2. Imaging flow cytometry measurement (**Figure 2**)
    1. Analyze the stained samples using an imaging flow cytometer at the flow cytometry core of Cincinnati Children's Hospital using a 40X objective to yield 300 pixels for a cell with around 10 mm in diameter. One-pixel size is approximately 0.5 mm by 0.5 mm of the object.
    2. Acquire 10,000 cellular images in an unbiased manner according to the manufacturer's instruction.

4. Imaging Analyses of Flow Cytometry Images

1. Colocalization analysis using IDEAS software (**Figure 2**)
    1. Perform compensation with single-stained versus non-stained samples by setting the fluorescence intensity of non-stained samples below the threshold, including non-stained BaP-exposed DCs with BaP autofluorescence, as in routine flow cytometry data analysis.
    2. Gate stained cells to obtain the subsets of HLA-$DR^+CD11c^+CD1d^+Lamp1^+$ cells (**Figure 2A**) and show cellular images in the gated subsets (**Figure 2B**).
    3. Save cell images in a png format based on two technical inclusion criteria, the visual presence of strong co-stained signals and subcellular localization of CD1d and Lamp1 proteins, for the colocalization analyses using ImageJ-Fiji (**Figure 2B**).

2. Use software ImageJ-Fiji to perform colocalization analysis (**Figure 3**).
    1. Prepare the input image files by merging the 100 saved cell images for non-exposed and BaP-exposed human DCs, respectively (**Figure 3A**).
    2. Analyze CD1d (Red) and Lamp1 (Green) colocalization using a scatterplot.
        1. Run ImageJ-Fiji program. Open the .png file with 100 cell images (**Figure 3B** and **Figure 4A**): *"File* | *Open"*.
        2. Split the image with merged red and green channels into two images with either a red or a green channel: *"Image* | *Color* | *Split channels"*.
        3. Draw a scatterplot using the commands *"Analyze* | *Colocalization* | *Colocalization Threshold"*. Save the scatterplot using the *"PrintScreen"* key.

    3. Calculate Mander's colocalization coefficients for each single cellular image (n=100) (**Figure 4B**)
        1. Select a single cell image on the image file with split channels using the "**Oval"** selection tool.
        2. Use the commands *"Analyze* | *Colocalization* | *Colocalization Threshold"*. Select *"Channel 1"* from the dialogue box of region of interest (ROI). Keep all calculation options including *"Mander's using thresholds"* for each cell image.
        3. Repeat this calculation for all 100 cell images.
        4. Save and open the results using a spreadsheet.
        5. Plot the average and standard errors for "thresholded Mander's coefficients" (n=100, 0 means no colocalization and 1 means perfect colocalization). Use Student's t-test to calculate the *p* value for the comparison between BaP-exposed and non-exposed groups (**Figure 4B**).

    4. Calculate the percent of thresholded pixel intensity co-localized between CD1d and Lamp1 for multiple cell images (n=100) (**Figure 4C**).
        1. Use the same analysis protocol in 4.2.3 and additionally select the result option *"% intensity above threshold colocalized"*.
        2. Perform this analysis together with Mander's colocalization coefficients.
        3. Similarly plot the average and standard errors for % intensity colocalized between CD1d and Lamp1. Use Student's t-test to calculate the *p* value for comparison between BaP-exposed and non-exposed groups (**Figure 4C**).

Representative Results

The lipophilic pollutant BaP alters endocytic gene clusters in human DCs. Human monocyte-derived DCs from each donor (n=3) were incubated with BaP and sorted for conventional DCs, which were further used for RNA extraction and transcriptomic analysis as described. Upon the normalization of gene expression, altered genes between BaP-exposed and non-exposed groups were clustered according to the functional correlation of differentially expressed genes. We input the altered gene list to the Toppcluster program[16] for the analyses of relevant cellular pathways and perform the statistical test using a false discovery rate (FDR) correction of *p* values (**Figure 1B**). Several major altered gene clusters, including lipid metabolism and endocytic functions, were identified in BaP-exposed DCs. In this study, we specifically focused on the functional test of endocytic trafficking, because CD1-mediated antigen presentation has been highly dependent on the lipid antigen loading in the endocytic pathway[5,19,20,21].

CD1d endocytic trafficking is demonstrated using imaging flow cytometry. Upon obtaining a large number of cell images using imaging flow cytometry, we started using the IDEAS program to visualize individual cellular images through conveniently gating cell populations co-stained with multiple antibodies (**Figure 2A**). Specifically, we were able to gate the major DC population co-stained with HLA-DR and CD11c to further show the DCs with CD1d and Lamp1 co-expression (**Figure 2A**). Co-stained signals can be enriched through gating the cell population with double stain of CD1d and Lamp1 (**Figure 2A**). We first showed the non-exposed normal DCs with minimal colocalization of CD1d and Lamp1 proteins, indicating the basal level of CD1d endocytic trafficking and high level of surface expression at physiological conditions (**Figure 2B**)[5,19,20,21]. To measure the colocalization of CD1d and Lamp1 proteins, we initially used IDEAS to show a slight increase of bright detail similarity between CD1d and Lamp1 proteins with BaP exposure[13]. The bright detail similarity was calculated based on the Pearson's correlation coefficient for testing the correlation of two factors, while CD1d and Lamp1 proteins were unlikely highly overlapped in physiological condition, indicating that CD1d is able to transiently traffic through late endocytic compartments to obtain functional lipid antigens. Thus, it is more biologically meaningful to test whether the CD1d protein in BaP exposure retains more in the late endocytic compartments as reflected by the increased percentage of overlapped CD1d and Lamp1 proteins using the imaging analysis software Fiji in the ImageJ package. Finally, retention of the CD1d protein in late endocytic compartments can be used to functionally confirm altered endocytic gene profiles in BaP exposure.

Co-localized intensity and area between CD1d and Lamp1 proteins was measured. To obtain a reproducible threshold setting and percentages of co-localized areas and intensity, we applied ImageJ-Fiji[22], which has also been used in several other studies[23,24,25]. We randomly select $CD1d^{+}Lamp1^{+}$ cells with strong co-stain and clear subcellular localization of CD1d and Lamp1 proteins as input images (**Figure 2B**). Individual cellular images can be merged to a single image file for one consistent analysis (**Figure 3A**). In our study, we merged 100 cell images and opened it in the program to analyze by setting "colocalisation thresholds" (**Figure 3B**). The colocalization of pixel intensity between two channels (PE-labeled CD1d and AF647-labeled Lamp1) was shown overall with a scatterplot by detecting the co-localized pixels from these 100 cell images (**Figure 4A**). In this plot, horizontal and vertical lines represent Costes's thresholds and the diagonal lines represent the ratio of overall pixel intensity between two channels. The Costes's threshold provides a visible setting for removing weak pixels from two overlapped channels. The resulted scatterplot shows an increased colocalization of CD1d and Lamp1 proteins in BaP exposure. Moreover, we quantified the degree of colocalization between CD1d and Lamp1 proteins using Mander's coefficients (**Figure 4B**). Consequently, Mander's coefficients demonstrate increased colocalization between CD1d and Lamp1 in late endocytic compartments of BaP-exposed DCs comparing with non-exposed DCs, as statistically supported by Student's t-tests (**Figure 4B**). However, if protein intensity is heterogeneous between colocalized and non-colocalized areas, colocalized intensity will be unparalleled to colocalized areas. Therefore, it is also necessary to further exam the colocalization based on intensity (**Figure 4C**). As a result, each column represents an averaged calculation of percentage of colocalized intensity from multiple cell images (n=100) between BaP-exposed and non-exposed conditions for a pair of co-localized proteins. Student's t-tests also show statistical significance (n=100, $p<0.001$) between BaP-exposed and non-exposed groups with indicated standard errors. Altogether, our data demonstrate that the CD1d protein was retained in late endosomes at BaP exposure, supporting that BaP-altered gene expression further leads to the impaired endocytic function and CD1d trafficking.

In summary, CD1d-Lamp1 colocalization enhances upon BaP exposure. Multiple parameters based on cell images (**Figure 2B**), including scatterplots with overlapped pixel intensity (**Figure 4A**), enhanced Mander's coefficients (**Figure 4B**), and increased percentage of overlapped intensity (**Figure 4C**), support CD1d endocytic retention at BaP exposure. This colocalization analysis of cellular images is an accurate approach to determine the degree of protein colocalization and demonstrate biological mechanisms of cell functions, for example, endocytic function consistent with disrupted endocytic gene expression, further contributing to the inhibited activation of CD1d-restricted T cells[13].

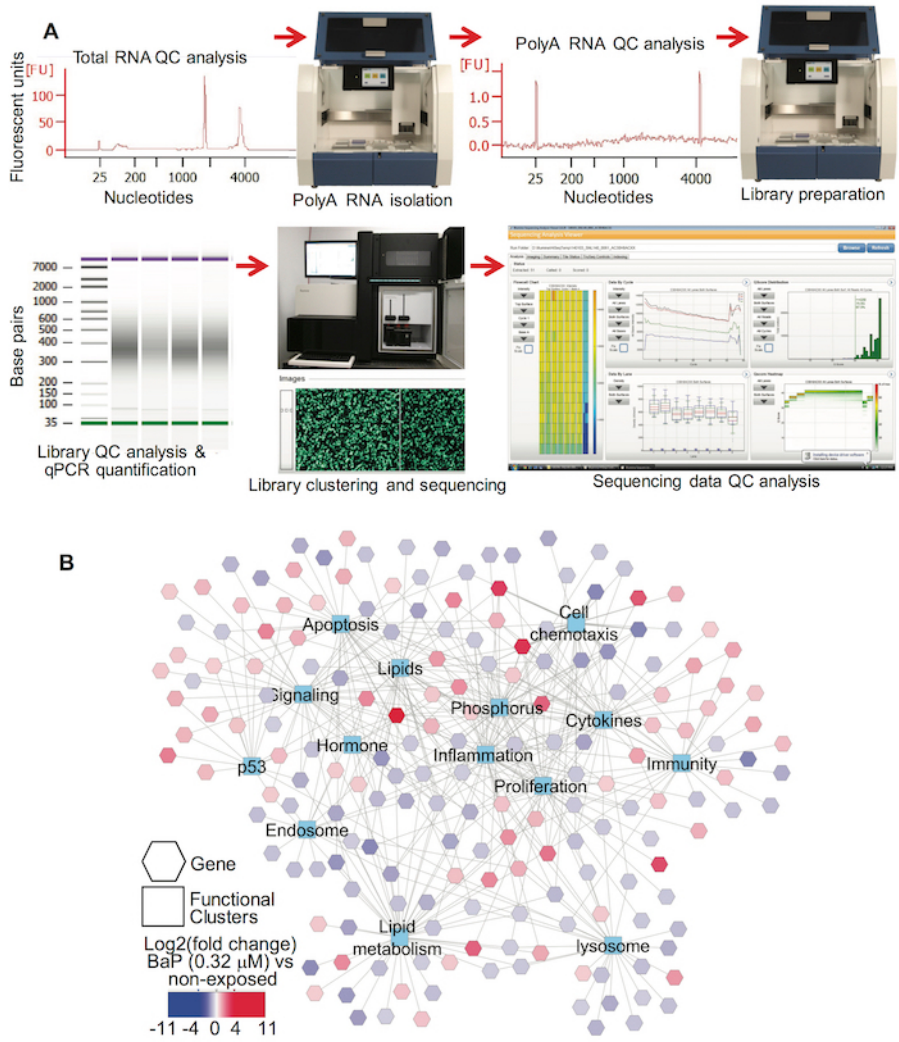

Figure 1: Perturbation of DC transcriptomes in BaP exposure (**A**) Flowchart of RNA-Seq. First, quality control (QC) analysis was performed to examine the quality of total RNA. Using an automated system and high-quality total RNA as input, poly-A RNA was isolated, which demonstrated depleted rRNA in poly-A RNA QC analysis. The poly-A RNA was then subjected to automated library preparation and indexing via PCR. Next, the amplified library was analyzed by a Bioanalyzer for QC with expected yield and size distribution. After qPCR quantification, indexed libraries were pooled and clustered onto flow cell for sequencing, and the sequencing data quality was real-time monitored. The axis represents relative counts of flow cytometry staining signals. **(B)** Altered genes were grouped in different functional clusters and the gene clusters associated with endocytic function and lipid metabolism are shown. Red: CD1d; Green: Lamp1. Please click here to view a larger version of this figure.

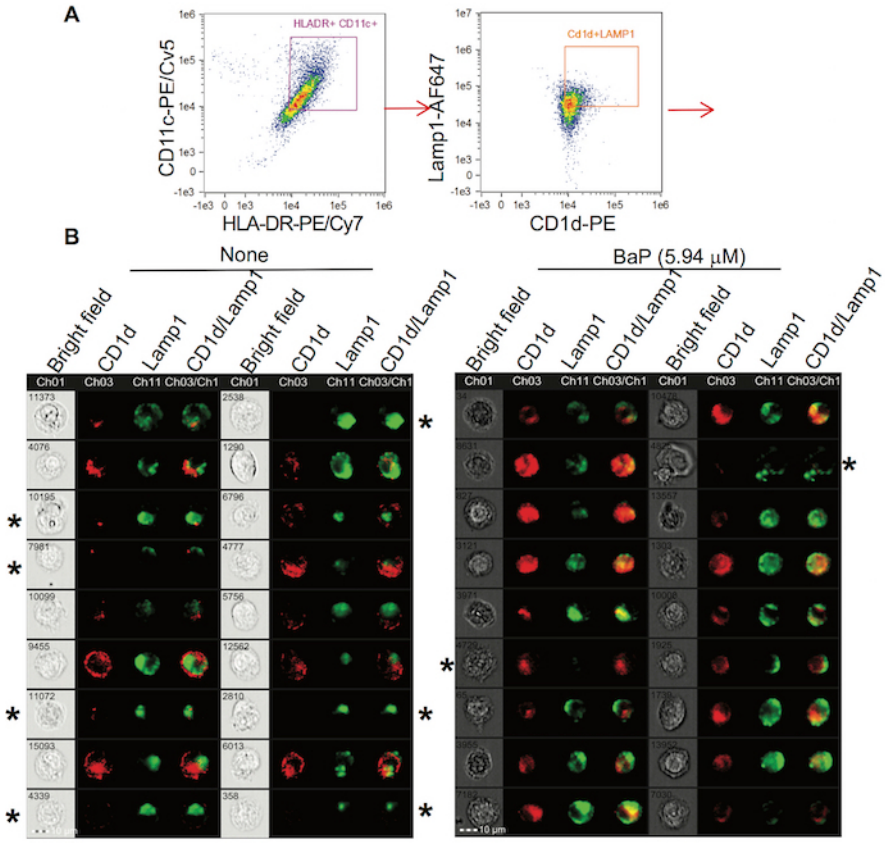

Figure 2: Analysis of cellular images using the IDEAS program. (**A**) Monocyte-derived DCs from healthy donors were firstly gated on HLA-DR+CD11c+ cells and further gated on $CD1d^{+}Lamp1^{+}$ cells using the IDEAS program. (**B**) Cellular images were extracted from the $HLA\text{-}DR^{+}CD11c^{+}CD1d^{+}Lamp1^{+}$ population for cellular image visualization. Please click here to view a larger version of this figure.

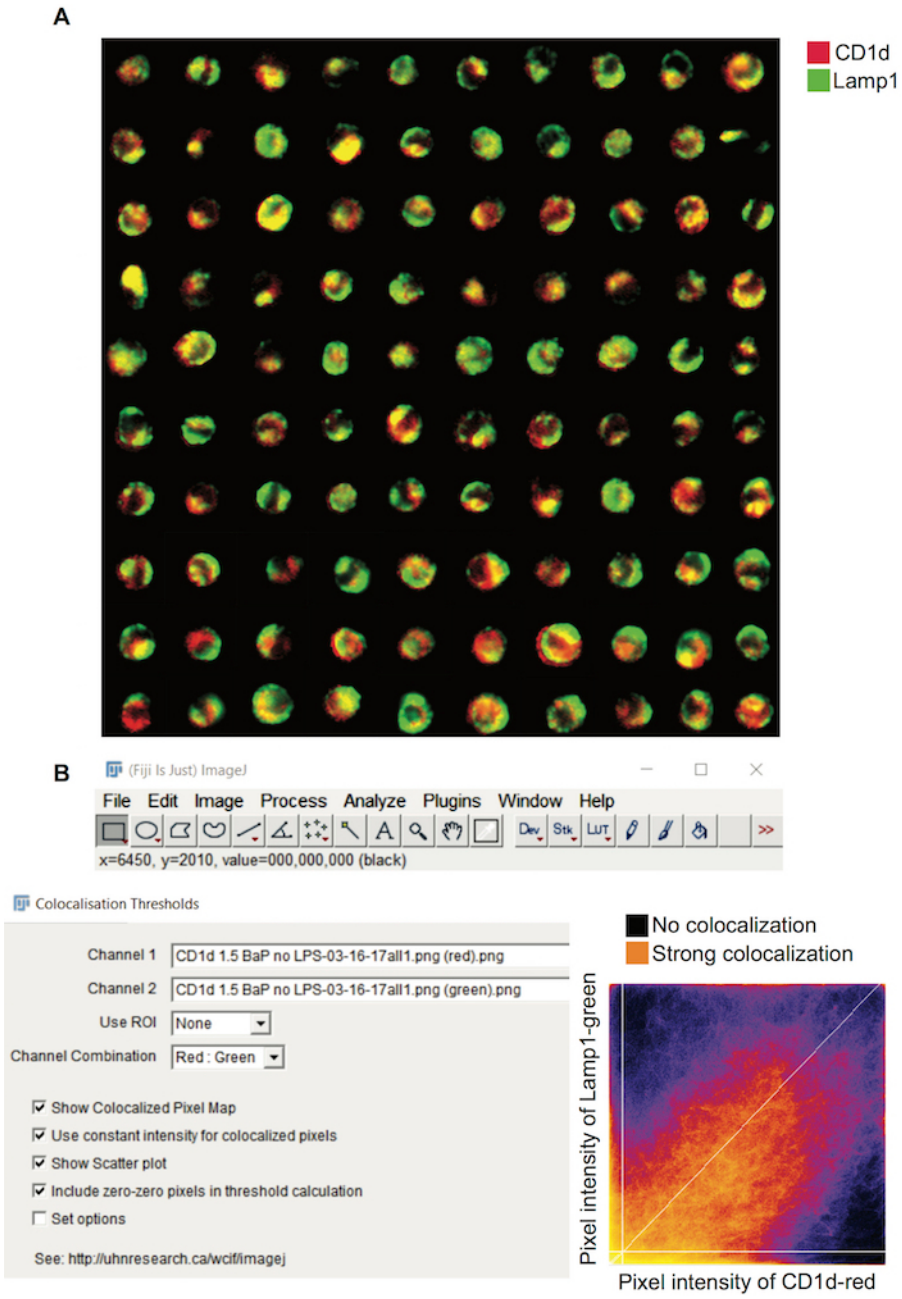

Figure 3: Analysis of cellular images using the Fiji-ImageJ program. Cells with strong co-stain of CD1d and Lamp1 proteins were randomly selected for the image analysis using Fiji-ImageJ, but cells* with invisible or weak staining for either CD1d or Lamp1 protein was excluded as in **Figure 2B**. (**A**) These randomly selected cellular images were assembled into a single image file as an input image. (**B**) The colocalization analysis was performed through setting the colocalization thresholds for both green and red channels. The scatterplots were generated with threshold calculation. Please click here to view a larger version of this figure.

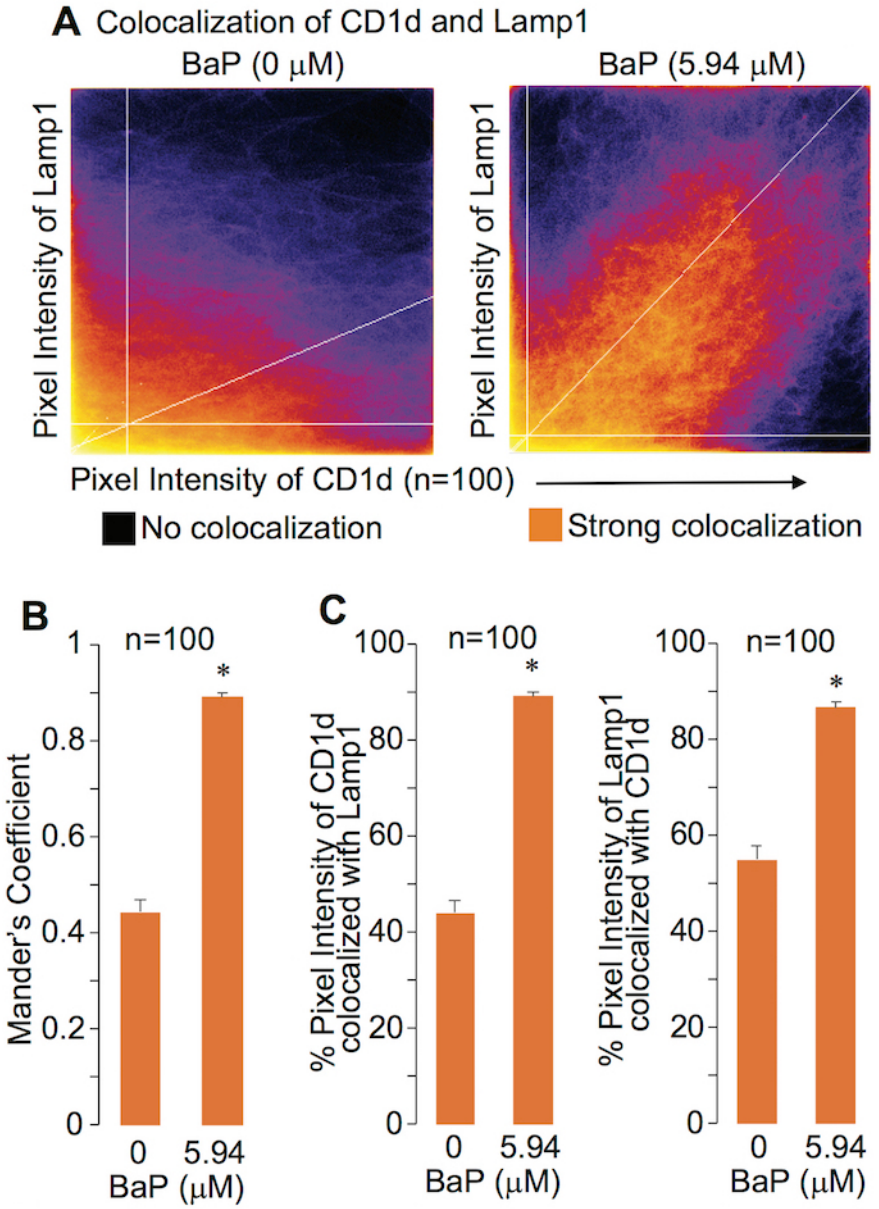

Figure 4: Colocalization of CD1d and Lamp 1 proteins. Using similar dataset reported in Sharma *et al.*[13], co-localized pixel intensity between CD1d and Lamp1 proteins from DCs at BaP-exposed and non-exposed conditions was recalculated and shown with scatterplots (**A**). Mander's coefficients for CD1d and Lamp1 colocalization were calculated and are shown with an average from selected cell images (**B**). The percentage of co-localized pixel intensity was also calculated (**C**). Statistical significance (n=100, p <0.001) was obtained with Student's t-tests in comparison to the non-exposed group. Standard errors were indicated. Data are from one assay with cells from a healthy donor. Two independent assays were performed with similar results. Please click here to view a larger version of this figure.

Antibodies	Fluorophores or secondary antibody	Clone
HLA-DR	Phycoerythrin/Cyanine 7 (PE/Cy7)	L243
CD11c	Phycoerythrin/Cyanine 5 (PE/Cy5)	3.9
CD1c	Brilliant violet 421	L161
Purified anti-human CD1d	PE-anti-mouse IgG2b	51.1
Lamp1	Alexa Fluor 647 (AF647)	CD107a(H4A3)

Table 1: Antibodies used in this study. Due to shared excitation and emission wavelengths, fluorophores PE/Cy5 and AF647 partially overlapped at staining signals. We use these fluorophores to label a surface protein (CD11c) and an intracellular protein (Lamp1) respectively to avoid their signal overlapping at a subcellular level. We also use optimal titration and compensation to minimize the overlapped signals between both fluorophores.

Discussion

Functional confirmation of an altered gene pathway is challenging, because of widely impacted gene expression involving multiple pathways and the difficulty to integrate individual and populational cellular activities. We employed imaging flow cytometry to specifically test CD1d trafficking in endocytic compartments. Imaging flow cytometry integrates the populational measurement of cells and the individual demonstration of subcellular colocalization of multiple proteins. Confocal microscopy has previously provided high resolution in measuring protein colocalization, and flow cytometry is able to provide comprehensive phenotyping for different cell populations. Imaging flow cytometry combines the advantages of confocal microscopy and flow cytometry at acceptable image resolution to analyze protein colocalization in a high-profile manner for functional confirmation of transcriptomic alteration by environmental pollutants.

Analyses of colocalization of multiple proteins in a populational scale are technically demanding, because (i) detailed analyses of multiple individual cells are labor-intensive and relatively biased; (ii) it is difficult to define an optimal threshold for interpreting overlapped pixels based on the intensity or area of positive staining; and (iii) balanced observation of individual and populational cells is critical. In this study, we focused on performing a biologically meaningful observation, a statistical significance test, and an imaging demonstration of co-localized proteins. To achieve this goal, we first obtained thousands of images of human DCs using imaging flow cytometry. Quantitative analyses of imaging files combined a bright detail similarity analysis using the software IDEAS and a statistically tested colocalization analysis using Fiji-ImageJ. The IDEAS program allows gating the co-stained population, calculating colocalization of two proteins using Pearson's correlation coefficient-based bright detail similarity, and randomly selecting co-stained cells with subcellular localization of proteins[13]. To further achieve the biological relevant demonstration of co-localized proteins, we used ImageJ-Fiji software and applied the Mander's coefficient to calculate the percentage of co-localized areas and overlapped pixel intensity to demonstrate the degree of CD1d localization in the endocytic pathway.

The critical step for using the ImageJ-Fiji program is to perform single cell imaging analysis. Variation of percentage protein colocalization from individual cells can be monitored in comparison to visually merged colors from single cell images. By averaging the percentage protein colocalization from all 100 cells, the means and standard errors can be calculated to demonstrate protein colocalization and functional correlation at a populational level. This bioinformatics analysis is simple and straightforward without concerning ambiguous results, because this analysis offers a reproducible threshold calculation using the Costes's method to produce the same resulted thresholds for the same data sets and similar thresholds for similar datasets[26]. The limitation of this technique is the labor-intensive manual input of single cell images and potentially subjective selection of visually co-stained cells using the IDEAs software. In our study, we analyze 100 cell images from each group and we set reproducible selection criteria, including strong co-stained signals and clear subcellular localization of CD1d and Lamp1 proteins. Overcoming these limitations requires technical improvement of analytical software to allow batch analysis and objective selection of single cells based on morphological features beyond the staining intensity provided by flow cytometry. In summary, combined cellular and population imaging analysis will provide highly reproducible, comprehensive, statistically tested, and biologically relevant results of percentage protein colocalization. We believe this CD1d-Lamp1 colocalization analysis can serve as a successful example of high profile cellular imaging analyses to answer broader questions on functional and morphological alteration of cellular proteins.

Disclosures

The authors have nothing to disclose

Acknowledgements

The authors thank Robert Giulitto (Hoxworth blood center) for human blood samples and Dr. Liang Niu for the normalization of gene expression reads. We also thank grant support from the National Institute of Environmental Health Sciences (ES006096), Center for Environmental Genetics (CEG) pilot project (S.H.), National Institute of Allergy and Infectious Diseases (AI115358) (S.H.), University of Cincinnati University Research Council award (S.H.), and University of Cincinnati College of Medicine Core Enhancement Funding (X. Z.).

References

1. Roche, P.A., Cresswell, P. Antigen Processing and Presentation Mechanisms in Myeloid Cells. *Microbiology Spectrum.* **4** (3) (2016).
2. Huang, S. *et al.* MR1 uses an endocytic pathway to activate mucosal-associated invariant T cells. *The Journal of experimental medicine.* **205** (5), 1201-1211 (2008).
3. Nakamura, N. *et al.* Endosomes are specialized platforms for bacterial sensing and NOD2 signalling. *Nature.* **509** (7499), 240-244 (2014).

4. Blum, J.S., Wearsch, P.A., Cresswell, P. Pathways of antigen processing. *Annual review of immunology.* **31**, 443-473 (2013).
5. Brennan, P.J., Brigl, M., Brenner, M.B. Invariant natural killer T cells: an innate activation scheme linked to diverse effector functions. *Nature reviews. Immunology.* **13** (2), 101-117 (2013).
6. Zajonc, D.M., Kronenberg, M. CD1 mediated T cell recognition of glycolipids. *Current opinion in structural biology.* **17** (5), 521-529 (2007).
7. Cox, D. *et al.* Determination of cellular lipids bound to human CD1d molecules. *PloS one.* **4** (5), e5325 (2009).
8. Yuan, W., Kang, S.J., Evans, J.E., Cresswell, P. Natural lipid ligands associated with human CD1d targeted to different subcellular compartments. *Journal of immunology.* **182** (8), 4784-4791 (2009).
9. Huang, S. *et al.* Discovery of deoxyceramides and diacylglycerols as CD1b scaffold lipids among diverse groove-blocking lipids of the human CD1 system. *Proceedings of the National Academy of Sciences of the United States of America.* **108** (48), 19335-19340 (2011).
10. de Jong, A. *et al.* CD1a-autoreactive T cells recognize natural skin oils that function as headless antigens. *Nature immunology.* **15** (2), 177-185 (2014).
11. Trombetta, E.S., Mellman, I. Cell biology of antigen processing *in vitro* and *in vivo*. *Annual review of immunology.* **23**, 975-1028 (2005).
12. Maecker, H.T., McCoy, J.P., Nussenblatt, R. Standardizing immunophenotyping for the Human Immunology Project. *Nature reviews. Immunology.* **12** (3), 191-200 (2012).
13. Sharma, M. *et al.* Inhibition of endocytic lipid antigen presentation by common lipophilic environmental pollutants. *Science Reports.* **7** (1), 2085 (2017).
14. Boom, R. *et al.* Rapid and simple method for purification of nucleic acids. *Journal of clinical microbiology.* **28** (3), 495-503 (1990).
15. Nachamkin, I. *et al.* Agilent 2100 bioanalyzer for restriction fragment length polymorphism analysis of the Campylobacter jejuni flagellin gene. *Journal of clinical microbiology.* **39** (2), 754-757 (2001).
16. Kaimal, V., Bardes, E.E., Tabar, S.C., Jegga, A.G., Aronow, B.J. ToppCluster: a multiple gene list feature analyzer for comparative enrichment clustering and network-based dissection of biological systems. *Nucleic acids research.* **38** (Web Server issue), W96-102 (2010).
17. Bauer-Mehren, A. Integration of genomic information with biological networks using Cytoscape. *Methods in molecular biology.* **1021**, 37-61 (2013).
18. Cline, M.S. *et al.* Integration of biological networks and gene expression data using Cytoscape. *Nature protocols.* **2** (10), 2366-2382 (2007).
19. Huang, S., Moody, D.B. Donor-unrestricted T cells in the human CD1 system. *Immunogenetics.* **68** (8), 577-596 (2016).
20. Huang, S. Targeting Innate-Like T Cells in Tuberculosis. *Frontiers in immunology.* **7**, 594 (2016).
21. Moody, D.B., Porcelli, S.A. Intracellular pathways of CD1 antigen presentation. *Nature reviews. Immunology.* **3** (1), 11-22 (2003).
22. Schindelin, J. *et al.* Fiji: an open-source platform for biological-image analysis. *Nature methods.* **9** (7), 676-682 (2012).
23. Diard, M. *et al.* Stabilization of cooperative virulence by the expression of an avirulent phenotype. *Nature.* **494** (7437), 353-356 (2013).
24. Bader, E. *et al.* Identification of proliferative and mature beta-cells in the islets of Langerhans. *Nature.* **535** (7612), 430-434 (2016).
25. Eliceiri, K.W. *et al.* Biological imaging software tools. *Nature methods.* **9** (7), 697-710 (2012).
26. Costes, S.V. *et al.* Automatic and quantitative measurement of protein-protein colocalization in live cells. *Biophysical journal.* **86** (6), 3993-4003 (2004).

